

Laser diffraction from capillary waves on liquid film surfaces*

ZHU Feng (朱峰)**, WANG Hong (王宏), CHEN Li-ju (陈利菊), and ZHANG Jian-hang (张建航)
Xi'an Communications Institute, Xi'an 710106, China

(Received 25 September 2012)

©Tianjin University of Technology and Springer-Verlag Berlin Heidelberg 2013

A simple experiment for laser diffraction of capillary waves on liquid film surface (LFS) is realized. Steady and visible diffraction patterns are obtained. The dispersion relation of capillary waves on LFS is verified by laser diffraction. In particular, both the relation between the wave number and the film thickness at a fixed angular frequency and the relation between the angular frequency and the wave number at a fixed film thickness are investigated. The theoretical and experimental results are in good agreement.

Document code: A **Article ID:** 1673-1905(2013)01-0065-4

DOI 10.1007/s11801-013-2361-7

Optical techniques have been available for investigation of surface waves since 1960s. For the surface wave at high frequencies, most techniques are based on the acoustic-wave diffraction, and the experiments were performed for ultrasonic waves^[1,2] since a higher surface wave frequency may cause a higher angular offset of diffraction. Surface waves on fluids, with wavelengths in the millimeter range or less, are known as capillary waves. Typically, the amplitude of these waves is of the order of one micrometer. In this regime, the dominant restoring force is the surface tension^[3,4]. G. Weisbuch^[5] and others^[6,7] considered capillary waves as a reflection diffraction grating for the laser beam, and light diffraction is capable of providing a variety of information of capillary waves on the single liquid surface. J. D. Barter^[8] adopted a capacitive antenna for the measurement of the dispersion relation of capillary waves on water surface. Our previous work^[9-13] described light diffraction from liquid surface waves at low frequency. However, there are few experiments performed to measure the dispersion relation of capillary waves on the liquid film surface (LFS).

In this paper, we describe a relatively simple method for the generation of capillary waves on LFS in the millimeter wavelength regime, and discuss a new technique for measuring their wavelength using light diffraction. The wavelength data provide a very reliable dispersion relation, which yields accurate values of the wave number for capillary waves on LFS. The dispersion relation of capillary waves on LFS is

verified by laser diffraction. In particular, both the relation between the wave number and the film thickness at a fixed angular frequency and the relation between the angular frequency and the wave number at a fixed film thickness are investigated. The theoretical and experimental results are in good agreement. In addition, the technique is easy to implement and real-time in nature.

A schematic diagram of the apparatus is shown in Fig. 1. A low frequency sinusoidal signal generator is used to produce an output at a few hundred of hertz, which is used to drive the capillary wave exciter. The wave exciter is a delicate triangle metal frame with its vertex connected to an electromagnetic rapping device. The exciter produces the plane wave on LFS. In addition, it is reasonable to assume that the frequency of capillary waves is the same as that of the exciter. The values of frequency are found directly from the frequency readings of the signal generator. A He-Ne laser beam ($\lambda = 632.8$ nm) is divided by using a beam splitter. One of the beams is used to monitor the laser output stability, and the other is directly incident on LFS where the capillary wave is traveling. The liquid pool with area of 936 cm² is put on a special plate and filled with distilled water to a depth of nearly 3 cm. The exciter is installed on a movable holder, so that the relative distance between the wave source and the incident point can be changed. A charge coupled device (CCD) imager (model MTV-1881EX) is used to detect the light distribution of the capillary wave in the region of the Fraunhofer

* This work has been supported by the National Natural Science Foundation of China (No.61102160), and the Natural Science Foundation of Xi'an Communications Institute (No.XTY-YXYJ-B-2012-17).

** E-mail: 2000zf36392@sina.com

or far-field diffraction. Because the screen is fairly far away (6.76 m in our case) from the diffraction center, the Fourier-transform lens is not used in our experimental setup. The data detected by the CCD are input into a computer. Of course, the diffraction patterns can be subsequently displayed, stored, and processed by the computer. The whole experimental setup including the optical system is set on an optical table equipped with pressurized air supports to minimize the possible effect of ambient vibrations. In experiment, an alcohol thermometer is used to measure the liquid temperature, and during our experiment, the recorded liquid temperature is 20 °C.

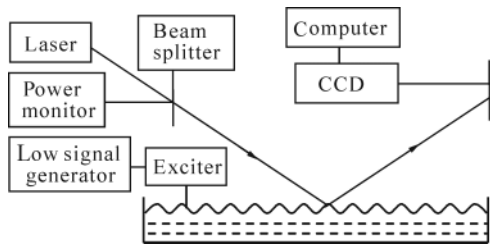


Fig.1 Schematic diagram of experimental setup

Though the surface particle motion is actually somewhat more complex in nature, capillary waves propagation can be adequately approximated as a traveling sinusoidal disturbance and written as

$$y = A \cos(\omega t - kx) , \quad (1)$$

where y is the displacement of the surface particle in the vertical direction, x is a variable along propagation direction of capillary waves, A is the amplitude, ω is the angular frequency, k is the wave number, and $k = 2\pi/\lambda_s$, where λ_s is the wavelength of capillary waves. As illustrated in Fig.2, it is assumed that a plane light wave is obliquely incident on LFS, which is disturbed by capillary waves with frequencies of a few hundred of hertz. LFS capillary waves appear as a reflection grating for the laser beam as shown in Fig.3, and produce the Fraunhofer diffraction patterns which are observed on a screen. The wavelength λ_s of capillary waves is the grating spacing. As depicted in Figs.2 and 3, the grating equation for both transmission and reflection is^[14]

$$\lambda_s [\cos \theta - \cos(\theta + \theta_m)] = m\lambda , \quad (2)$$

where θ is the grazing angle of incidence beam. To increase the diffraction efficiency, the grazing angle θ is chosen to be as small as reasonably possible. In our experiment, θ is 0.09 rad. θ_m is the diffraction angle of the m th-order spot. Each integer m represents the order number of the various principal maxima. λ is the wavelength of the laser. The grating equation Eq.(2), for the first-order spot $m = \pm 1$, becomes

$$\lambda_s [\cos \theta - \cos(\theta + \theta_1)] = \lambda , \quad (3)$$

and

$$\lambda_s [\cos \theta - \cos(\theta - \theta_1)] = -\lambda . \quad (4)$$

Using Eqs.(3) and (4), we obtain

$$\lambda_s \sin \theta \sin \theta_1 = \lambda , \quad (5)$$

where θ_1 is diffraction angle of the first-order spot as shown in Fig.2, $\sin \theta = h/\sqrt{h^2 + l^2}$ and $\sin \theta_1 \approx d/(2\sqrt{h^2 + l^2})$, where h is the perpendicular height of the zeroth-order spot from LFS level, l is the horizontal distance between the location of the laser spot on LFS and the screen, and d is the distance between the positive and the negative first-order diffraction spots on the screen. In our experiment, $h = 0.56$ m, and $l = 6.76$ m. Thus, using Eq.(5) we get

$$k = 2\pi/\lambda_s = \pi h d / \lambda (h^2 + l^2) . \quad (6)$$

In our experiment, CCD captures diffraction patterns on the screen, and d is measured by computer. To reduce the systematic error of d , we measure d at least three times. The values of d are obtained through averaging these data. Using Eq.(6) we get the values of k . A careful and accurate measurement of d with the order of a few millimeters is crucial for evaluating k .

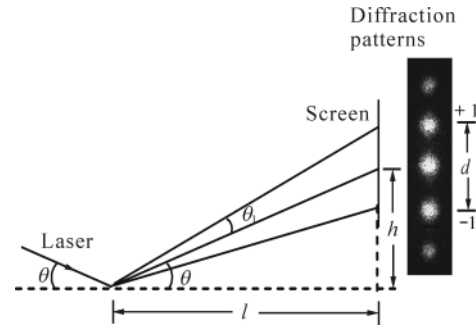


Fig.2 Principle of light diffraction from LFS capillary waves

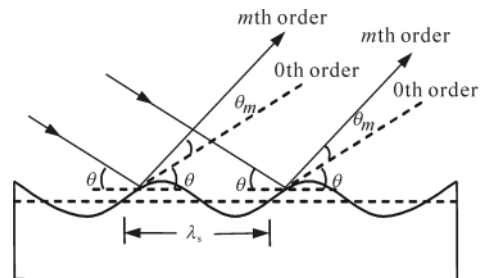


Fig.3 A reflection LFS grating

When the depth of liquid is large, the dispersion relation of capillary waves on the single liquid surface is taken as^[15] $\omega_0^2 = \alpha_0 k_0^3 / \rho_0$, where ω_0 and k_0 are the angular frequency and the wave number of capillary waves on the single liquid

surface, α_0 and ρ_0 are the surface tension and the density of the liquid, respectively. When there exists a film of a different liquid on top of the given liquid, the two liquids are immiscible, and the depth of the lower liquid is large, the dispersion relation of capillary waves on the upper LFS becomes^[16]

$$\omega^2 = \frac{E + \sqrt{G}}{2F}, \quad (7)$$

where we neglect a term due to gravity, and use the notations of $E = r\omega_1^2 + \omega_1^2 \tanh(kh') + \omega_2^2$, $F = 1 + r \tanh(kh')$, $G = E^2 - 4F\omega_1^2\omega_2^2 \tanh(kh')$, $r = \rho'/\rho$, $\omega_1^2 = \alpha'k^3/\rho'$ and $\omega_2^2 = \alpha k^3/\rho$ for simplicity, where ω and k are the angular frequency and the wave number of the capillary wave on LFS, respectively, ρ' is the density of the upper liquid film, α' is the surface tension at the film-air interface, ρ ($\rho' < \rho$) is the density of the lower liquid, α is the interfacial tension at the liquid-film interface, and h' is the thickness of the liquid film. Let us first assume $h' \rightarrow \infty$ (i.e., $kh' \gg 1$), then $\omega^2 \rightarrow \omega_1^2$. On the contrary, assuming $h' \rightarrow 0$ (i.e., $kh' \ll 1$), we get $\omega^2 \rightarrow (\gamma\omega_1^2 + \omega_2^2) = (\alpha + \alpha')k^3/\rho$.

According to Eqs.(6) and (7), as the angular frequency ω or film thickness h' is changed, the distance d and wave number k also change. In addition, it is reasonable to assume that the angular frequency ω of capillary waves is the same as that of the exciter which is driven by a signal generator. Thus, the values of ω are found directly from the frequency readings of the signal generator. The dispersion relation of capillary waves on LFS can be measured by using the known frequencies, the film thickness h' and the wave number k .

In our experiments, we choose films of kerosene and benzene spread on the surface of the distilled water. The choice of these liquids is due to the fact that they are immiscible with water, and their densities are lower than that of water. Because the liquid film is formed by adding a measured quantity of the second liquid in drops from a hospital injector, we can measure the volume of the liquid film within 0.1 ml. The thickness of the film is estimated from the known volume of the liquid and the surface area of the pool. In order to avoid any decrease of thickness due to evaporation, we observe the formation of the uniformly spread film within 5 min.

Fig.4 shows the theoretical plots of the wave number k versus the film thickness h' for kerosene at a fixed frequency of 220 Hz and benzene at a fixed frequency of 200 Hz using Eq.(7). Experimentally measured data are also shown in Fig.4. Here, we use standard values of kerosene^[17] as $\alpha' = 28.5$ mN/m, $\alpha = 36.5$ mN/m, $\rho' = 800$ kg/m³, and the density of water $\rho = 1000$ kg/m³ in Eq.(7) at a temperature of 20 °C. Similarly, we use standard values of benzene as $\alpha' = 28.9$ mN/m, $\alpha = 35.0$ mN/m, $\rho' = 870$ kg/m³, and the density of water $\rho = 1000$

kg/m³ in Eq.(7) at 20 °C. As the film thickness h' changes, the distance d between the positive and the negative first-order diffraction spots on the screen also changes. Sets of diffraction patterns are obtained on the screen for different values of h' . The volume of the liquid is increased from 2.5 ml to 60 ml, i.e., the thickness of the liquid film is increased from 2.67×10^{-5} m to 6.41×10^{-4} m, at a fixed frequency of 220 Hz for kerosene and 200 Hz for benzene. CCD captures the corresponding diffraction pattern of each volume. The distance d between the positive and the negative first-order spots is measured by computer. Hence, using Eq.(6), we estimate the value of k for a particular h' . The experimental result matches well with the theoretical curve. It can be seen in Fig.4 that for film thickness less than 5×10^{-4} m, (i.e., 0.5 mm), the wave number rapidly increases with increase of the film thickness, but for film thickness greater than 0.5 mm, the wave number slowly changes with change of the film thickness.

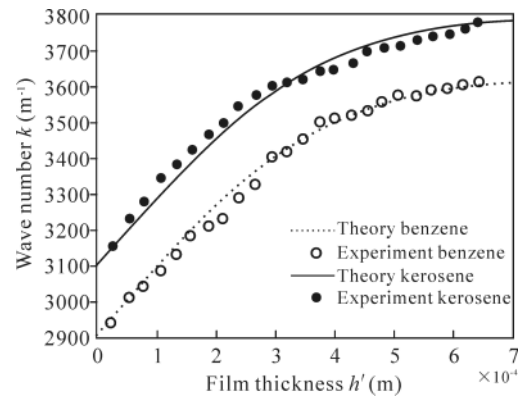


Fig.4 Wave number k versus the film thickness h' on LFS

Fig.5 shows theoretical plots of the angular frequency ω versus the wave number k at a fixed film thickness of 1.603×10^{-4} m for kerosene and 2.137×10^{-4} m for benzene using Eq.(7) at 20 °C. Experimentally measured data are also shown. As described in the previous section, here we use standard values α' , α , ρ' , and ρ in Eq.(7). As the angular frequency ω changes, the distance d between the positive and the negative first-order diffraction spots on the screen also changes. Sets of diffraction patterns are obtained on the screen for different values of ω . In our experiment, the frequency of capillary waves is increased from 80 Hz to 280 Hz, i.e., the angular frequency of capillary waves is increased from 502.7 Hz to 1759.3 Hz at a fixed film thickness of 1.603×10^{-4} m for kerosene and 2.137×10^{-4} m for benzene. CCD captures the corresponding diffraction pattern of each frequency. The distance d is measured by computer. Hence, using Eq.(6), we estimate the value of k for a particular ω . As shown in Fig.5, theoretical curves perfectly match with experimental results.

Light diffraction from LFS is experimentally realized. Diffraction from capillary waves on LFS is used to investi-

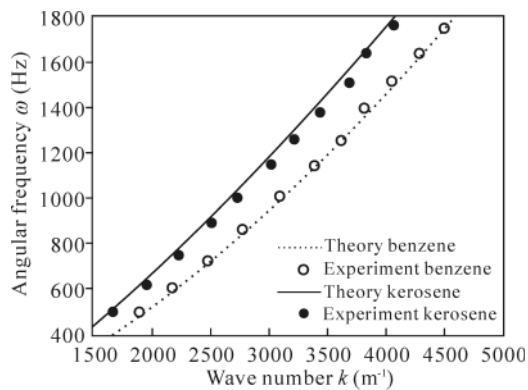


Fig.5 Angular frequency ω versus the wave number k on LFS

gate the dispersion relation on LFS. Highly visible stationary diffraction patterns are obtained from LFS. We verify the dispersion relation of capillary waves on LFS with experiments. Experimental data agree well with theoretical curves. Moreover, we note that this technique can easily be used to measure the film thickness, which appears in the dispersion relation. Our technique is easy to implement and noncontact in nature. In order to avoid any decrease of thickness due to evaporation, experiment should be completed rapidly.

References

- [1] F. Behroozi, J. Smith and W. Even, *American Journal of Physics* **78**, 1165 (2010).
- [2] X. M. Chen, B. H. Yang, X. G. WU and Y. Z. Wu, *Optoelectronics Letters* **7**, 291 (2011).
- [3] Z. B. Hou, X. H. Zhao and J. H. Xiao, *European Journal of Physics* **33**, 199 (2012).
- [4] F. Behroozi and A. Perkins, *American Journal of Physics* **74**, 957 (2006).
- [5] G. Weisbuch and F. Garbay, *American Journal of Physics* **47**, 355 (1979).
- [6] L. Zhang, F. Miao, Q. M. Sui, D. J. Feng, H. P. Liu and H. L. Liu, *Journal of Optoelectronics • Laser* **23**, 897 (2012). (in Chinese)
- [7] R. Fan, C. P. Tang and M. Deng, *Journal of Optoelectronics • Laser* **22**, 1067 (2011). (in Chinese)
- [8] J. D. Barter, *Review of Scientific Instruments* **64**, 556 (1993).
- [9] J. Dong, R. C. Miao and J. X. Qi, *Journal of Applied Physics* **100**, 033108 (2006).
- [10] F. Zhu, R. C. Miao and C. L. Xv, *American Journal of Physics* **75**, 896 (2007).
- [11] J. Dong, J. X. Qi and R. C. Miao, *Brazilian Journal of Physics* **37**, 1129 (2007).
- [12] F. Zhu, R. J. Luo, Y. P. Xue and R. C. Miao, *Journal of Optoelectronics • Laser* **20**, 847 (2009). (in Chinese)
- [13] R. C. Miao, N. N. Li, M. L. Gao and P. B. Han, *Acta Photonica Sinica* **40**, 828 (2011). (in Chinese)
- [14] M. Born and E. Wolf, *Principles of Optics*, 7th ed., Beijing: Higher Education Press, 2005.
- [15] P. G. Klemens, *American Journal of Physics* **52**, 451 (1984).
- [16] ЛДЛАНДАУ and Е.М. ЛИФШИЦД, *Fluid Mechanics*, Beijing: Higher Education Press, 1983. (in Chinese)
- [17] G. Q. Liu, L. X. Ma and J. Liu, *Handbook of Chemical Industry and Physics*, Beijing: Chemical Industry Press, 2002. (in Chinese)